SE8100003

COSMIC AND SUBATOMIC PHYSICS REPORT
LUIP 8008
NOVEMBER 1980
LUNFD6/NFFK-7008)1-20(1980)
ISSN 0348-9329

HIGH-SPIN BAND STRUCTURE IN ^{166}Yb.

W. MALUŚ, N. ROY, S. JÖNSSON, L. CARLÉN AND H. RYDE
DEPARTMENT OF PHYSICS, UNIVERSITY OF LUND,
SÖLVEGATAN 14, S-223 62 LUND, SWEDEN.

G.B. HAGEMANN, B. HERSKIND, J.D. GARRETT AND Y.S. CHEN,
THE NIELS BOHR INSTITUTE,
BLEGDAMSVEJ 17, DK-2100 COPENHAGEN, DENMARK.

J. ALMBERGER AND G. LEANDER,
DEPARTMENT OF MATHEMATICAL PHYSICS,
LUND INSTITUTE OF TECHNOLOGY,
SÖLVEGATAN 14A, S-223 62 LUND, SWEDEN.

COSMIC AND SUBATOMIC PHYSICS
UNIVERSITY OF LUND
SÖLVEGATAN 14
S-223 62 LUND, SWEDEN

HIGH-SPIN BAND STRUCTURE IN ^{166}YB.

W. WALUŚ, N. ROY, S. JÓNSSON, L. CARLÉN AND H. RYDE
DEPARTMENT OF PHYSICS, UNIVERSITY OF LUND,
SÖLVEGATAN 14, S-223 62 LUND, SWEDEN.

G.B. HAGEMANN. B. HERSKIND, J.D. GARRETT AND Y.S. CHEN,
THE NIELS BOHR INSTITUTE,
BLEGDAMSVEJ 17, DK-2100 COPENHAGEN, DENMARK.

J. ALMBERGER AND G. LEANDER,
DEPARTMENT OF MATHEMATICAL PHYSICS,
LUND INSTITUTE OF TECHNOLOGY,
SÖLVEGATAN 14A, S-223 62 LUND, SWEDEN.

High-spin band structure in ^{166}Yb.

W. Waluś*, N. Roy, S. Jönsson, L. Carlén and H. Ryde,
Department of Physics, University of Lund,
Sölvegatan 14, S-223 62 LUND, Sweden.

G.B. Hagemann, B. Herskind, J.D. Garrett and Y.S. Chen**,
The Niels Bohr Institute,
Blegdamsvej 17, DK-2100 COPENHAGEN, Denmark.

J. Almberger*** and G. Leander,
Department of Mathematical Physics,
Lund Institute of Technology,
Sölvegatan 14A, S-223 62 LUND, Sweden.

Abstract.

High-spin states in ^{166}Yb have been studied via the ^{154}Sm(^{16}O,4n)^{166}Yb reaction with 80 MeV ^{16}O ions from the NBI tandem accelerator. γ-γ coincidence data were accumulated with an array of four Ge(Li) and four NaI(Tl) detectors to favour high multiplicity events. Totally about $3 \cdot 10^8$ events were accumulated in the coincidence experiment. Measurements of the angular distribution of the γ-radiation and the conversion coefficients were furthermore performed. Four weakly populated side bands are observed besides the yrast cascade which is followed up to its 24^+ member. The ground state band has thus been identified to its 18^+ state, while the crossing Stockholm band becomes the yrast band from its 16^+ member. The S-band is established from its 12^+ state. The observed level energies and transition rates are well reproduced in calculations within the particle rotor model.

---

* On leave of absence from the Jagellonian University, Cracow, Poland.

** On leave of absence from the Institute of Atomic Energy, Peking, China.

*** Research Institute of Physics, Stockholm, Sweden.

1. Introduction.

In the mass region A = 150-170 the S-(Super or Stockholm)band[1] built upon aligned $(\nu i_{13/2})^2$ orbits, usually crosses the ground state band (g.s.b.) around spin 14 and may cause backbending, depending upon the interaction between the g.s. and S-band. The interpretation of the band structure and band crossings in rotational nuclei along the lines of Bohr and Mottelson[1] provides us with a means to compare experimental results with a microscopic theory and to extract quantities like the crossing frequency and the aligned angular momentum from the experimental data. The nucleus ^{166}Yb is of special interest, because a priori it would seem to be one of the best rotors which can be significantly populated at very high spins by (HI,xn) reactions. The identification of discrete lines in this work extends the information about the non-yrast bands from lighter and less rotational-like nuclei, and furthermore complements the gamma correlation work described elsewhere in these proceedings[2].

2. Experimental technique and results.

States in ^{166}Yb were populated following the ^{154}Sm(^{16}O,4n)^{166}Yb reaction at a beam energy of 80 MeV, the beams being provided by the NBI tandem accelerator. The experiments consisted of γ-ray angular distribution, γ-γ coincidence and conversion electron coefficient measurements. The reaction yields at this bombarding energy, with an isotopically enriched, metallic target of ^{154}Sm sputtered to a thickness of 1.5 mg/cm^2 onto a lead backing, were about 77% ^{166}Yb, 15% ^{165}Yb and 7% ^{167}Yb.

2.1. Singles γ-ray measurements

With the target at an angle of 45° relative to the beam direc-

tion two sets of singles γ-ray spectra were obtained at 5 different angles, one with a Ge(Li) detector at angles ranging between 58° and 148° and the other with a Ge(Li) detector in a Compton-suppression set-up at angles between 0° and 90°. One stationary Ge(Li) detector placed below the target served as the monitor. In spite of the low counting rate, the data for the weak transitions obtained with the anti-Compton set-up proved to be superior to those with the other detector due to the reduced background. Efficiency calibrations at various angles were performed with a radioactive ^{152}Eu source placed at the target position. A typical spectrum obtained with the anti-Compton set-up at 90° is shown in fig. 1. Two sets of angular distribution coefficients were obtained, one for each detector, by fitting the peak intensities to the expression $W(\theta) = A_0 + A_2P_2(\cos\theta) + A_4P_4(\cos\theta)$, after normalizing them to the monitor yields and correcting for the dead times of the ADC:s and the variations of the relative efficiency at different angles. The results from the two detector set-ups are consistent. The results of the angular distribution measurements are summarised in table 1. The energy calibration was done by recording a singles γ-ray spectrum at 90° along with the spectrum from a ^{152}Eu source placed near the target.

2.2. γ-γ coincidence measurements.

γ-γ coincidence measurements were performed with an array of four Ge(Li) detectors and four NaI(Tℓ) detectors. The gains of the amplifiers of the Ge(Li) detectors were matched to be equal. Only those coincidence events were accumulated on magnetic tape for off-line analysis, for which two Ge(Li) counters in addition to at least one of the remaining Ge(Li) detectors or one of the NaI(Tℓ) detectors were triggered. In

all, about 300 million pairs of events were accumulated. The tapes were sorted for all the possible combinations of pairs of detectors and the resulting spectra, after background subtraction, were added together. Examples of coincidence spectra are shown in fig. 2. In a similar coincidence run for studying the ^{167}Yb nucleus with a 80 MeV ^{17}O beam, the yield of ^{166}Yb was about 50% with no observable yield found for ^{165}Yb. As many transitions in ^{165}Yb have the same or nearly the same energy as those in ^{166}Yb, the data from the latter experiment helped to remove ambiguities concerning many weak transitions and to confirm the level scheme of ^{166}Yb.

2.3. Conversion coefficient measurements.

In order to ascertain the multipolarities of the transitions, the conversion electron spectrum was obtained at 55° with a solenoid transporter and a cooled Si(Li) detector. The electron intensities were recorded in the range from about 600 keV to about 1200 keV as this region contained most of the interband transitions. A γ-ray-spectrum was also recorded simultaneously at -55°. The conversion coefficients were normalized to the α_K(E2) values of the 603,710 and 722 keV transitions The results of the conversion coefficients measurements have led to the assignment of negative parity of two side bands.

3. Construction of the level scheme

The yrast sequence of levels in ^{166}Yb was earlier known up to spin 20^+. Many low-lying levels up to an excitation energy of 2.43 MeV are known from the radioactive decay studies[3] of ^{166}Lu. The level scheme of ^{166}Yb, as deduced from the present work, is presented in fig. 3. Previously known levels, not seen in this work, are not included in the figure. The spin

and parity assignments are based on the angular distribution and conversion coefficient measurements with frequent reference to previous measurements. All the transitions within a band are found to be of stretched E2 character. The ordering of the transitions within a band is based on their coincidence relationships and their relative intensities.

3.1. The ground state and S-bands

The yrast sequence of levels has been extended up to a spin of 24^+ and the g.s.b. to a spin of 18^+. Although the 667 and 739 keV lines, depopulating the 22^+ and the 24^+ levels, respectively, show considerable Doppler broadening,their angular anisotropies are well enough determined and have the same magnitude as expected for stretched E2 transitions high up in a cascade, and thereby justify their assignments. The 356 keV transition from the $12^{+'}$ to the 12^+ state could only be inferred from the coincidence data. Its intensity, the angular distribution coefficients and hence the M1/E2 mixing ratio could not be determined due to the presence of a contaminant line from the radioactive decay of the reaction products. The intensity of the 592 keV 16^+ to $14^{+'}$ state transition could only be inferred from the coincidence data due to the presence of another transition having nearly the same energy.

3.2. The odd-spin negative parity band.

One band with odd-spin and negative parity has been identified. The 11^- member of this band and the higher lying members are joined by a cascade of stretched quadrupole transitions and connected to the g.s.b. by four interband transitions. The measured K-conversion coefficient of the 688 keV transition

confirms the negative parity assignment of this band. The intensity ratios of the intraband transitions to the interband transitions to the g.s.b. decrease going down the band. The intraband transitions among the 5^-, 7^-, 9^- and the 11^- states at 1790, 1959, 2209 and 2417 keV are too weak to be detected in the coincidence work. The 5^- and 7^- states are known from the work of de Boer et al.[3]. The stretched E1 character of the transition from the 9^- state to the 8^+ member of the g.s.b. is established from angular distribution and conversion coefficient measurements.

3.3. The even-spin negative parity band.

The level at 1865 keV, which lies at the bottom of the even-spin negative parity band, has been observed in the radioactive decay of ^{166}Lu (ref.[3]) and assigned a spin and parity of 6^-. The regularity and the stretched E2 character of the cascade transitions populating this level justify the classification of this cascade as a band. Furthermore, the state 10^- at 2361 keV decays by an intense, mixed transition to the level at 2209 keV, which is assigned as having spin and parity 9^- in this study. This mixed transition is assumed to be of the M1/E2 type. Multipole admixture of higher order than quadrupole would require the level at 2361 keV to be an isomer with a lifetime of the order of microseconds.

3.4. The γ-vibrational band.

Several members of the γ-vibrational band have been observed earlier in the radioactive decay of ^{166}Lu (ref.[3]). The 5^+ member of this band is populated rather strongly in the present study and the angular distribution and the conversion electron data confirm the 5^+ assignment. The 2^+_γ and 3^+_γ levels

are populated very weakly and we infer their presence in this study from the observed branching ratios of the decays of these levels. The 7^+ level at 1705 keV has been found to decay by a stretched M1 transition to the 6^+ state of the g.s.b. It is to be noted that this level is not the same as the 7^+ level found earlier[3]. The assignment of the higher lying members of this band is only tentative and is based upon the observed decay properties of these levels, the systematic variation of the level differences and the similarity to the N=96 isotone ^{166}Er.

3.5. An unassigned rotational band and further levels.
A band of levels of unknown spins and parity and built on the 1835 keV state is observed in the present study. This band is connected by means of three weak interband transitions to the proposed γ-vibrational band, and the energies of these transitions are too close to strong g.s.b. transitions to make a determination of their multipole character possible in the present experiment. The tentatively suggested spins and negative parity are based on the observation of a similar band in ^{166}Er starting in that case with spin (8) at an excitation energy of 2091 keV.

The levels at 1617, 1957 and 2233 keV (cf. Fig. 3) are known from the work of de Boer et al.[3]. Our identification of these levels is based solely on the observation of some transitions originating from these levels in our coincidence spectra Only these transitions are shown in fig. 3 and other decay modes of these levels, not established in the present study, are excluded from the figure.

4. Theoretical considerations

A crossing of two bands is sometimes referred to as virtual or real, depending on whether or not an interaction between the two bands is likely to deflect a gamma cascade from one band to another. The real crossing known in the deformed rare-earth nuclei all occur between bands which do not interact because of different signature or parity. The crossings between the g.s. and S-bands, on the other hand, are generally virtual and an yrast cascade tends to stay yrast. However, it is illustrated by the case of ^{166}Yb that even when the interaction between the bands is not forbidden, there may be situations when the nucleus prefers to follow a band of given structure rather than the trajectory of lowest energy. In section 4.1 the general conditions for such behaviour are formulated in terms of the band parameters. In section 4.2 it is pointed out that the different cascade patterns in the two N=96 isotones ^{164}Er and ^{166}Yb arise naturally in particle-rotor calculations based on the notion of $(\nu i_{13/2})^2$ bands crossing the ground band. Section 4.3 contains a phenomenological analysis in terms of cranking model quantities for the positive and negative parity bands shown in fig. 3.

4.1. Two-band analysis.

A schematic model can be used to derive the conditions when a crossing between two weakly interacting bands is mainly virtual or mainly real. The energies of the two unperturbed bands as functions of the spin I are written

$$E = A_i(I-J_i)^2 + E_i^0 \qquad i = 1,2$$

They cross at a spin I_c. The difference J_2-J_1 between the aligned spins is denoted j. Perturbed bands are obtained by

diagonalizing a two by two matrix with an off-diagonal matrix element V. It is then straightforward to find the perturbed energies and the relative transition rates. The branching ratio of the transition rates from the lowest state of spin I to the upper and lower states of spin (I-2) are, in two special cases

$$\frac{T(I_c \to I_c-2)}{T(I_c \to (I_c-2)')} = \left[\frac{1}{1-\frac{j}{I_c}}\right]^5 + O(V)$$

and

$$\frac{T(I_c+1 \to I_c-1)}{T(I_c+1 \to (I_c-1)')} = \frac{V}{A_j}\left[\frac{1-\frac{1}{2}\frac{j}{I_c}}{1-\frac{j}{I_c}}\right]^5 + O(V^2),$$

respectively. In the first case the bands cross at one of the discrete spins where states exist, and it is seen that the yrast cascade tends to remain yrast. In the second case, where the bands cross in between the discrete states, the yrast cascade tends to leave the yrast line if V is sufficiently small. For given A and j this situation is clearly favoured by a large spin I_c.

A two-band analysis along the lines of ref.[4] for the energy levels of ^{164}Er and ^{166}Yb is described in sect. 4.3 below. It gives $I_c \sim 16$ in the former nucleus and $I_c \sim 15$ in the latter which thus accounts for the observed difference in the gamma cascade of the two nuclei. Other parameters obtained from the two-band analysis are the interaction V between the two unperturbed bands, and the inertia parameters. The branching ratios of the decays of the g.s. and the S-band suggest an in-

teraction V of the order ot 45-50 keV.

4.2. Particle-rotor analysis.

It has recently been shown[5,6] that the many-BCS-quasiparticle plus rotor Hamiltonian within a $(i_{13/2})^2$ valence space can be adjusted to give an accurate description of the energies along the g.s. and S-bands of ^{164}Er and ^{166}Yb. If the energies are correct it is expected that the calculation also accounts for branching ratios, and in particular the observed differences between the two nuclei in this respect. For ^{166}Yb the adjustable parameters[5] (θ_o = 35.463 MeV^{-1}, C = 0.0039308 MeV^3, λ = 0.0545 MeV above $\epsilon_{5/2}$ and Δ =0.669952 MeV) were fitted in ref.[5] to the yrast levels of spin I = 0-20, so the energies of all non-yrast levels, and, furthermore, the branching ratios can be regarded as predictions of the model. A calculated branching of the yrast cascade at I=16 has been reported earlier[7].

A comparison between results of the model calculations and experiments is given for the two nuclei in fig. 4 and table 2. The energies of the non-yrast levels in ^{166}Yb are of course not quite as well reproduced as in ^{164}Er, where levels from the high-spin continuation of the g.s.-band and the low-spin continuation of the S-band were included in the parameter fitting procedure. Nevertheless, the calculation is sufficiently accurate to describe the branching of the electromagnetic decay, cf. table 3. The transitions following the unperturbed bands through the crossing are indeed significantly stronger for ^{166}Yb than for ^{164}Er. Thus the transition from 16^+ to $14^{+'}$ has been seen in the ^{166}Yb case but not in ^{164}Er. A decay branch from the $12^{+'}$ level to the 12^+ level as well as to

the 10^+ level is measured in ^{166}Yb. The $12^{+'}$ to 12^+ transition is of particular interest because, according to the calculation, it is an almost pure M1 from the S-band to the g.s.-band. The parameters employed here for calculating the electromagnetic transition rates are Q = 7b, $e^{eff} = e$, $g_s^{eff} = 0.6\, g_s^{free}$, $g_\ell = 0$ and $g_R = Z/A$. A complication which should be noted is that the observed $12^{+'}$ level comes 9 keV below the calculated one, and just as in ^{164}Er, this may indicate an admixture of the 12^+ level from the gamma band[8].

4.3. Cranking model analysis.

The alignment plots[9] for the various bands are shown in fig. 5. The g.s. and the other bands except the S-band, are fitted with the parameters[9] $\mathcal{J}_0 = 29$ MeV$^{-1}\hbar^2$ and $\mathcal{J}_1 = 136$ MeV$^{-3}\hbar^4$. The corresponding parameters for the S-band have been adjusted to give a constant value of i_x above the backbend and are $\mathcal{J}_0 = 33.5$ MeV$^{-1}\hbar^2$ and $\mathcal{J}_1 = 62.5$ MeV$^{-3}\hbar^4$. The fact that the same values of the moment of inertia parameters generally do not give constant alignment values both below and above the backbend has been discussed by Bengtsson[10] and is probably due to the changes in the core associated with the backbending effect. The g.s. and S-bands show up with nearly constant alignments after correction for their mutual interaction, which is assumed to be constant and equal to 50 keV. The point corresponding to the $18^+ \rightarrow 16^+$ g.s.b. transition shows upbending, which is due to a crossing with the S'-band in the particle-rotor calculation.

The experimental Routhians are shown in fig. 6. The S-band Routhian crosses that of the g.s.b. at $\hbar\omega = 0.28$ MeV. The odd-spin odd parity band shows regular behaviour only above spin 11^-. This band and the even-spin negative parity

band built on the 6^- state at 1865 keV could be the two lowest bands with $\alpha = 1$ and 0 respectively, built on the neutron levels labelled $\left[642\frac{5}{2}\right]$ and $\left[523\frac{5}{2}\right]$ at zero frequency[9].

The extrapolated experimental Routhians for these bands cross the g.s. band at $\hbar\omega \approx 0.36$ MeV. No concrete assignments have been made for the band with the band head at 1835 keV. The spin of the band head is probably 6. If this is the case, then this band could be the other $\alpha = 0$ even-spin negative parity band based on the same neutron quasiparticle configuration as mentioned above. It may be noted, however, that the lowest identified member of a similar band in N = 96 isotone ^{164}Er has been assigned a spin (8) and has been suggested[9] to belong to the neutron configuration $\left[642\frac{5}{2}\right]\left[505\frac{11}{2}\right]$ K = 8.

5. Conclusions.

Judging by the first few states of the g.s. band, the nucleus $^{166}Yb_{96}$ is more appropriately classified as a stably deformed rotational nucleus than the more neutron-deficient rare-earth isotopes. Previously the only high-spin levels known were the yrast levels up to spin 20 (ref.11). In the present work six bands are identified, up to spin 24 on the yrast line and up to 23 in one of the side bands, thereby extending the systematics of high-spin band structure into the region of well-deformed nuclei. Many of the states were also populated and assigned similar spins and parities in a parallel study of the ^{162}Dy (^{9}Be,5n)^{166}Yb reaction at Brookhaven[12]. The positive-parity bands are presumably aligned neutron $(i_{13/2})^2$ configurations and the negative-parity bands could be neutron $(i_{13/2})(h_{11/2})$ configurations[9]. The VMI parameters, Routhians and values for the aligned angular momentum are extracted

from the data. A gamma correlation experiment[13] has also been made recently, which reaches the very high-spin states in the isotopes around ^{166}Yb, and the information obtained in the present work about the detailed spectroscopy up to spins above 20 should be a valuable aid in the interpretation of the results[2,14].

The crossing between the g.s. and S-band of ^{166}Yb has a special feature. It is the first known case of a crossing between two interacting bands in deformed rare-earth nuclei where a significant fraction of the cascade intensity leaves the trajectory of the lowest energy in order to follow an unperturbed band characterized by intrinsic structure. The mechanism is a small interaction combined with a band crossing spin in between the even integer values where there are physical states. Heating of the nucleus by this mechanism may occur more frequently for band crossings at higher spins. A number of interband transitions are observed in the present case at and just below the crossing, which provide more of a test for theory than the data on other backbending rare-earth nuclei. The levels and the M1 and E2 transitions matrix elements obtained from an $(i_{13/2})^2$ plus rotor calculation, made before the experiment and fitted to the energies along the yrast line, turn out to be consistent in detail with the observed energies and intensities.

Acknowledgements.

We wish to express our sincere thanks to the Nordic Committee for Acceleratorbased Research for financial support.

References

1. Bohr, A. and Mottelson, B.R., Proc. Int. Conf. on Nuclear Structure, Tokyo (1977)

2. Deleplanque, M.A., these proceedings

3. de Boer, F.W.N., Goudsmit, P.F.A., Koldewijn, P. and Meyer, B.J., Nuclear Physics A225, 317 (1974)

4. Bengtsson, R. and Frauendorf, S., Nuclear Physics A314, 27 (1979)

5. Almberger, J., Hamamoto, J. and Leander, G., Nuclear Physics A333, 184 (1980)

6. Almberger, J., Hamamoto, J. and Leander, G., Physica Scripta, in press

7. Chen, Y.S., Garrett, J.D., Almberger, J. and Leander, G., Physics Letters 94B, 468 (1980)

8. Johnson, N.R., Cline, D., Yates, S.W., Stephens, F.S., Riedinger, L.L. and Ronningen, R.H., Phys. Rev. Letters 40, 151 (1978)

9. Bengtsson, R. and Frauendorf, S., Nuclear Physics A327, 139 (1979)

10. Bengtsson, R., to be published in J. de Phys.

11. Lederer, C.M., and Shirley, V.S., Table of Isotopes, 7th edition, John Wiley & Sons, New York, N.Y. (1978)

12. Sunyar, A.W., private communication

13. Herskind, B., private communication

14. Leander, G., Chen, Y.S. and Nilsson, B.S., these proceedings.

Table 1.

The energies, intensities and angular distribution coefficients for the transitions assigned to ^{166}Yb following the ^{154}Sm(^{16}O,4n)^{166}Yb reaction at 80 MeV.

E_γ [a] (keV)	Intensity [b]	Ang.dist.coeff. [c] A_2/A_0	A_4/A_0	I_i^π [d] → I_f^π [d]
102.2		0.27(03)	-0.06(03)	$2^+ \rightarrow 0^+$
114				$8^- \rightarrow 7^-$
152				$10^- \rightarrow 9^-$
206[e]	16	0.21(07)	-0.05(08)	$8^- \rightarrow 6^-$
228.1	987	0.30(03)	-0.09(03)	$4^+ \rightarrow 2^+$
248[e]	8			$6^- \rightarrow (4^-)$
274[e]	weak			$(7^-) \rightarrow (7^-)$
276[e]	weak			$(7^-) \rightarrow (6^+)$
289[e]				$(4^-) \rightarrow 5^+$
289.4	55	0.30(02)	-0.10(02)	$10^- \rightarrow 8^-$
301.4	14	0.42(05)	0.02(05)	$(8^-) \rightarrow (6^-)$
337.5	1000	0.32(03)	-0.11(03)	$6^+ \rightarrow 4^+$
341	weak			$(10^-) \rightarrow 9^+$
354.4	28	0.28(03)	-0.03(04)	$(10^-) \rightarrow (8^-)$
356[e]	16			$12^{+\prime} \rightarrow 12^+$
366[e]	5	0.29(02)	-0.15(02)	$14^{+\prime} \rightarrow 12^{+\prime}$
367.6[e]	65			$12^- \rightarrow 10^-$
368[e]				$(7^-) \rightarrow 6^-$
375.8	37	0.27(02)	-0.12(03)	$16^{+\prime} \rightarrow 14^{+\prime}$
400.4	51	0.34(03)	-0.10(03)	$(12^-) \rightarrow (10^-)$
403[e]	17			$17^- \rightarrow 16^+$
430.2	856	0.31(03)	-0.13(03)	$8^+ \rightarrow 6^+$
432[e]	weak			$(8^-) \rightarrow 7^+$

Table 1.
(con't.)

E_γ (keV)	Intensity	Ang.dist.coeff. A_2/A_0	A_4/A_0	$I_i^\pi \rightarrow I_f^\pi$
437.6	63	0.27(03)	-0.08(03)	$14^- \rightarrow 12^-$
445.8[e]	33	0.14(09)	-0.02(07)	$13^- \rightarrow 11^-$
446[e]				$9^+ \rightarrow 7^+$
459.4	27	0.36(05)	-0.19(05)	$(14^-) \rightarrow (12^-)$
490.8	43	0.32(06)	-0.07(09)	$15^- \rightarrow 13^-$
494.3	128	0.35(01)	-0.09(01)	$16^{+'} \rightarrow 14^+$
496.7	22	0.38(04)	-0.18(05)	$(11^+) \rightarrow 9^+$
499.5	45	0.33(03)	-0.13(03)	$16^- \rightarrow 14^-$
507.7	645	0.32(08)	-0.09(01)	$10^+ \rightarrow 8^+$
508[e]				$(6^-) \rightarrow 5^+$
509[e]	160	0.23(03)	-0.11(03)	$18^{+'} \rightarrow 16^{+'}$
527.5	14	0.26(07)	-0.01(11)	$(16^-) \rightarrow (14^-)$
538[e]	19	-0.26(24)	-0.16(25)	$6^- \rightarrow 5^+$
538.2[e]	35	0.47(13)	0.04(14)	$17^- \rightarrow 15^-$
550[e]	15	0.22(04)	0.03(07)	$13^+ \rightarrow 11^+$
552.8	32	0.20(05)	-0.03(08)	$18^- \rightarrow 16^-$
569.7	480	0.33(03)	-0.11(03)	$12^+ \rightarrow 10^+$
575.1	17	-0.30(18)	0.15(17)	$15^- \rightarrow 14^+$
586.2[c]	30	0.22(07)	0.34(09)	$19^- \rightarrow 17^-$
588.4	69	0.36(05)	-0.02(08)	$20^{+'} \rightarrow 18^{+'}$
592[e]	14	0.27(17)	-0.07(22)	$16^+ \rightarrow 14^{+'}$
592[e]	10			$(18^-) \rightarrow (16^-)$
600.1	25	0.25(12)	0.05(13)	$20^- \rightarrow 18^-$

Table 1.

(con't.)

E_γ (keV)	Intensity	Ang.dist.coeff. A_2/A_0	Ang.dist.coeff. A_4/A_0	$I_i^\pi \rightarrow I_f^\pi$
603.5	250	0.31(02)	-0.13(02)	$14^+ \rightarrow 12^+$
629[e]	24	0.29(03)	-0.05(07)	$(6^+) \rightarrow 5^+$
630[e]				$21^- \rightarrow 19^-$
649[e]	10			$22^- \rightarrow 20^-$
649[e]	weak			$(20^-) \rightarrow (18^-)$
660[e]	7			$5^+ \rightarrow 6^+$
667	25	Doppler broadened		$22^{+\prime} \rightarrow 20^{+\prime}$
674[e]	13	0.13(09)	-0.33(09)	$23^- \rightarrow 21^-$
687.8	45	-0.21(02)	0.10(03)	$13^- \rightarrow 12^+$
701				$18^+ \rightarrow 16^+$
709[f]	4			$\rightarrow 4^+$
710.3	39	0.34(03)	-0.02(05)	$16^+ \rightarrow 14^+$
722.0	69	0.35(01)	-0.05(02)	$14^{+\prime} \rightarrow 12^+$
739		Doppler broadened		$24^{+\prime} \rightarrow 22^{+\prime}$
811.6	39	-0.15(07)	0.01(06)	$11^- \rightarrow 10^+$
830[f]	22			$2^+ \rightarrow 2^+$
860	10			$(7^-) \rightarrow 8^+$
925.6	15	0.27(05)	-0.16(07)	$12^{+\prime} \rightarrow 10^+$
932[f]	21			$2^+ \rightarrow 0^+$
936[f]	16			$3^+ \rightarrow 2^+$
997.3	38	-0.19(03)	0.15(07)	$5^+ \rightarrow 4^+$
1037	22	-0.31(06)	0.05(07)	$7^+ \rightarrow 6^+$
1053	16	-0.31(07)	0.03(08)	$9^+ \rightarrow 8^+$
1111.2	19	-0.22(04)	0.04(05)	$9^- \rightarrow 8^+$
1122	8			$(5^-) \rightarrow 6^+$

Table 1

(con't.)

E_γ (keV)	Intensity	Ang.dist.coeff. A_2/A_0	Ang.dist.coeff. A_4/A_0	$I_i^\pi \rightarrow I_f^\pi$
1290	25	-0.19(04)	0.06(04)	$(7^-) \rightarrow 6^+$
1460[e]				$(5^-) \rightarrow 4^+$

a) Energy uncertainties are 0.2 keV for strong transitions (rel.int. > 50), rising to 0.5 keV for weaker transitions.

b) Intensities are given relative to the $6^+ \rightarrow 4^+$ g.s.b. transition.

c) Only fitting errors are given.

d) Assignments in brackets are tentative.

e) Weak or doublet. Intensities wherever given for individual transitions, are based on the coincidence data, uncorrected for the angular correlation effects.

f) Lines known from the decay of ^{166}Lu. Assignments are based on the observed branching ratios.

Table 2.

Comparison of the theoretical and experimental level energies for the g.s. and S-bands of ^{164}Er and ^{166}Yb. The calculated energies are shown in brackets alongside the experimental values.

	^{164}Er				^{166}Yb			
	g.s.b.		S-band		g.s.b.		S-band	
0^+	0	(0)			0	(0)		
2^+	91.3	(91.5)			102.2	(101.9)		
4^+	299.4	(299.9)			330.3	(330.1)		
6^+	614.3	(615.1)			667.8	(667.8)		
8^+	1024.5	(1025.0)			1098.0	(1097.8)		
10^+	1517.9	(1518.0)			1605.7	(1605.3)		
12^+	2082.5	(2082.7)	2519.0	(2527.3)	2175.4	(2176.4)	2531.3	(2522.1)
14^+	2702.2	(2702.4)	2874.4	(2866.6)	2778.9	(2779.3)	2897.4	(2890.5)
16^+	3411.2	(3413.0)	3262.6	(3255.0)	3489.2	(3499.1)	3273.2	(3271.9)
18^+	4121.5	(4122.2)	3768.1	(3767.1)	4190	(4196.6)	3782	(3786.6)
20^+	4868.2	(4865.5)	4345.3	(4350.7)			4370	(4370.0)
22^+			4999.3	(5005.0)			5038	(5018.0)
24^+			5728.1	(5724.9)			5777	(5725.0)

Table 3.

Comparison of the theoretical and experimental B(E2) and B(M1) ratios for g.s. and S-bands of ^{164}Er and ^{166}Yb.

	^{166}Yb		^{164}Er	
	th.	exp.	th.	exp.
$\frac{B(E2,\ 16^+ \to 14^+)}{B(E2,\ 16^+ \to 14^{+'})}$	1:1.3	1:0.9	1:0.6	---
$\frac{B(E2,\ 16^{+'} \to 14^{+'})}{B(E2,\ 16^{+'} \to 14^+)}$	1:1.2	1:0.9	1:0.5	1:0.4
$\frac{B(E2,\ 14^+ \to 12^+)}{B(E2,\ 14^+ \to 12^{+'})}$	5.2:1	---	35:1	---
$\frac{B(E2,\ 14^{+'} \to 12^{+'})}{B(E2,\ 14^{+'} \to 12^+)}$	4.4:1	2.1:1	24:1	22:1
$\frac{B(M1,\ 12^{+'} \to 12^+)}{B(E2,\ 12^{+'} \to 10^+)}$	2000:1	1600:1	1200:1	1250:1

Figure captions

Fig. 1. Singles γ-ray spectrum at 90° to the beam direction, using an anti-Compton set-up, taken during bombardment of a ^{154}Sm target with 80 MeV ^{16}O,

Fig. 2. Ge(Li) γ-γ coincidence spectra (background - subtracted) observed following the ^{154}Sm(^{16}O,4n)^{166}Yb reaction at 80 MeV.

Fig. 3. Level scheme of ^{166}Yb showing states populated by the ^{154}Sm(^{16}O,4n)^{166}Yb reaction.

Fig. 4. Comparison of the theoretical and experimental level energies for the g.s. and S-bands of ^{164}Er and ^{166}Yb. The calculated energies are shown below the experimental values.

Fig. 5. Plot of the alignment versus rotational frequency for the various bands in ^{166}Yb. The g.s. and the other bands except the S-band are fitted with the parameters[9] $\mathcal{J}_0 = 29$ MeV$^{-1}\hbar^2$ and $\mathcal{J}_1 = 136$ MeV$^{-3}\hbar^4$. The corresponding parameters for the S-band have been adjusted to give a constant value of i_x above the backbending and are $\mathcal{J}_0 = 33.5$ MeV$^{-1}\hbar^2$ and $\mathcal{J}_1 = 62.5$ MeV$^{-3}\hbar^4$.

Fig. 6. Experimental Routhians for the various bands in ^{166}Yb.

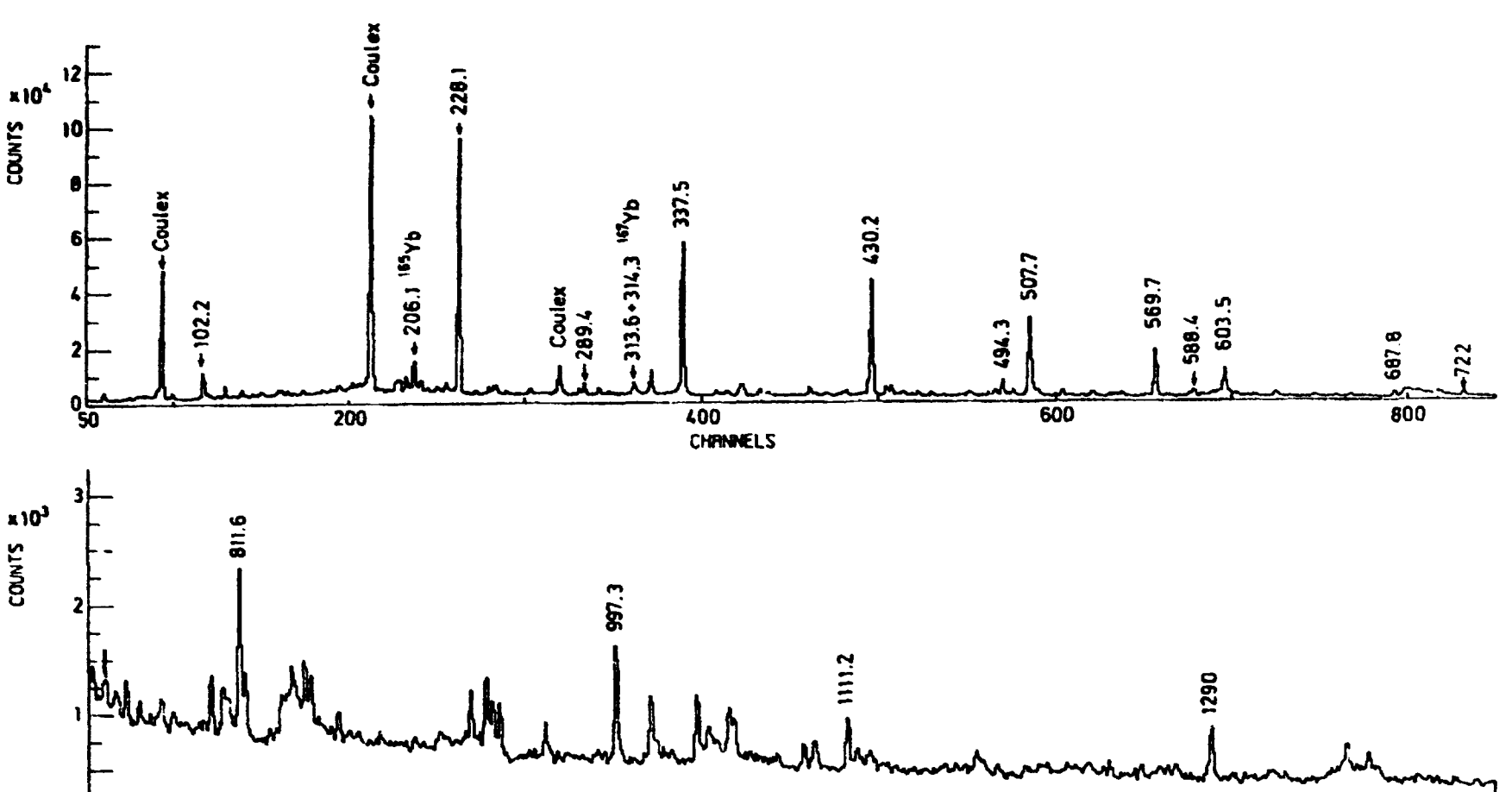
COUNTS x10⁴
Coulex
102.2
Coulex
206.1 ¹⁶⁵Yb
228.1
Coulex
289.4
313.6+314.3 ¹⁶⁷Yb
337.5
430.2
494.3
507.7
569.7
588.4
603.5
687.8
722
CHANNELS
COUNTS x10³
811.6
997.3
1111.2
1290
CHANNELS

Fig.1

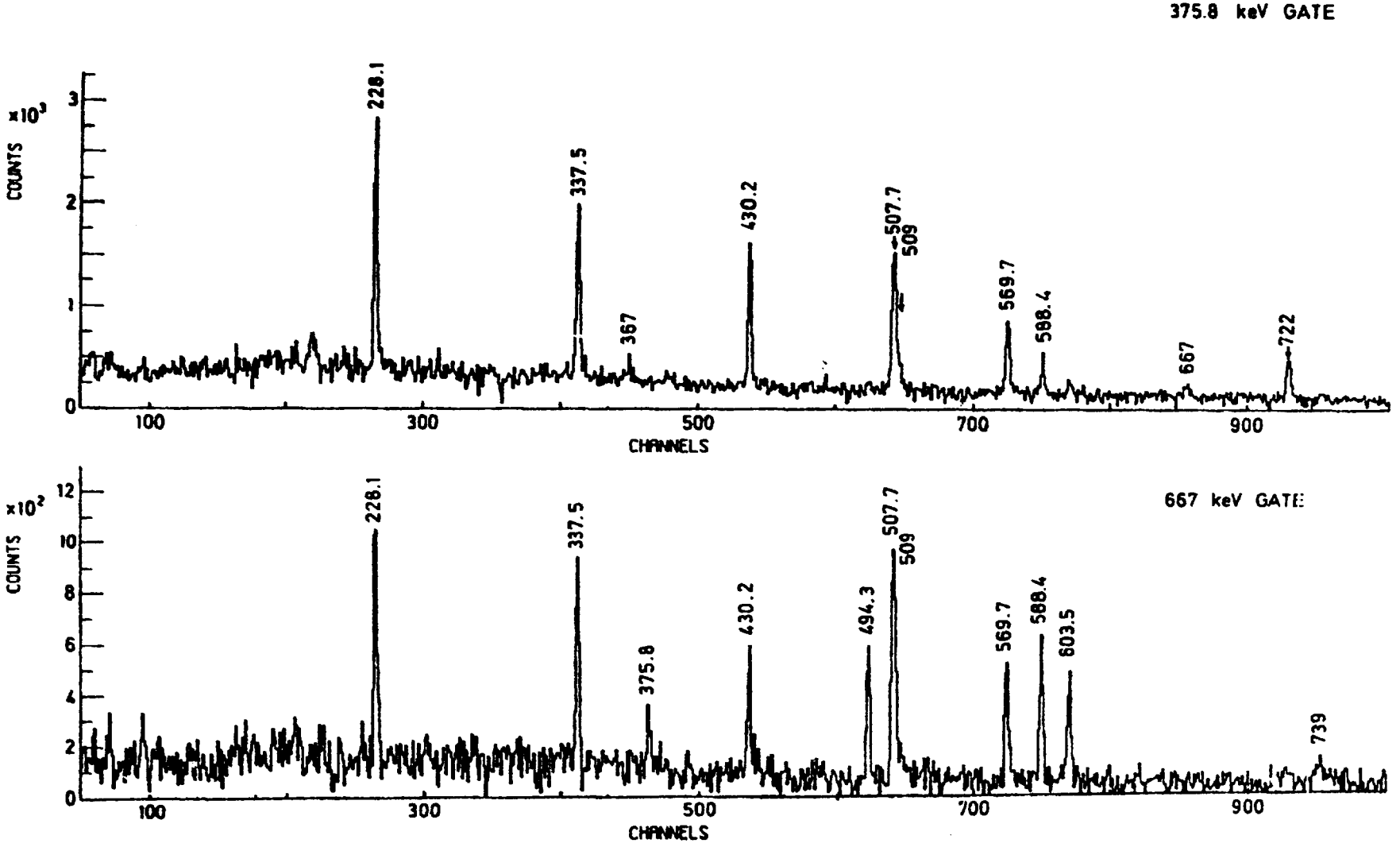
375.8 keV GATE
COUNTS
x10³
228.1
337.5
367
430.2
507.7
509
569.7
588.4
667
722
CHANNELS
667 keV GATE
x10²
228.1
337.5
375.8
430.2
494.3
507.7
509
569.7
588.4
603.5
739
CHANNELS

Fig. 2.

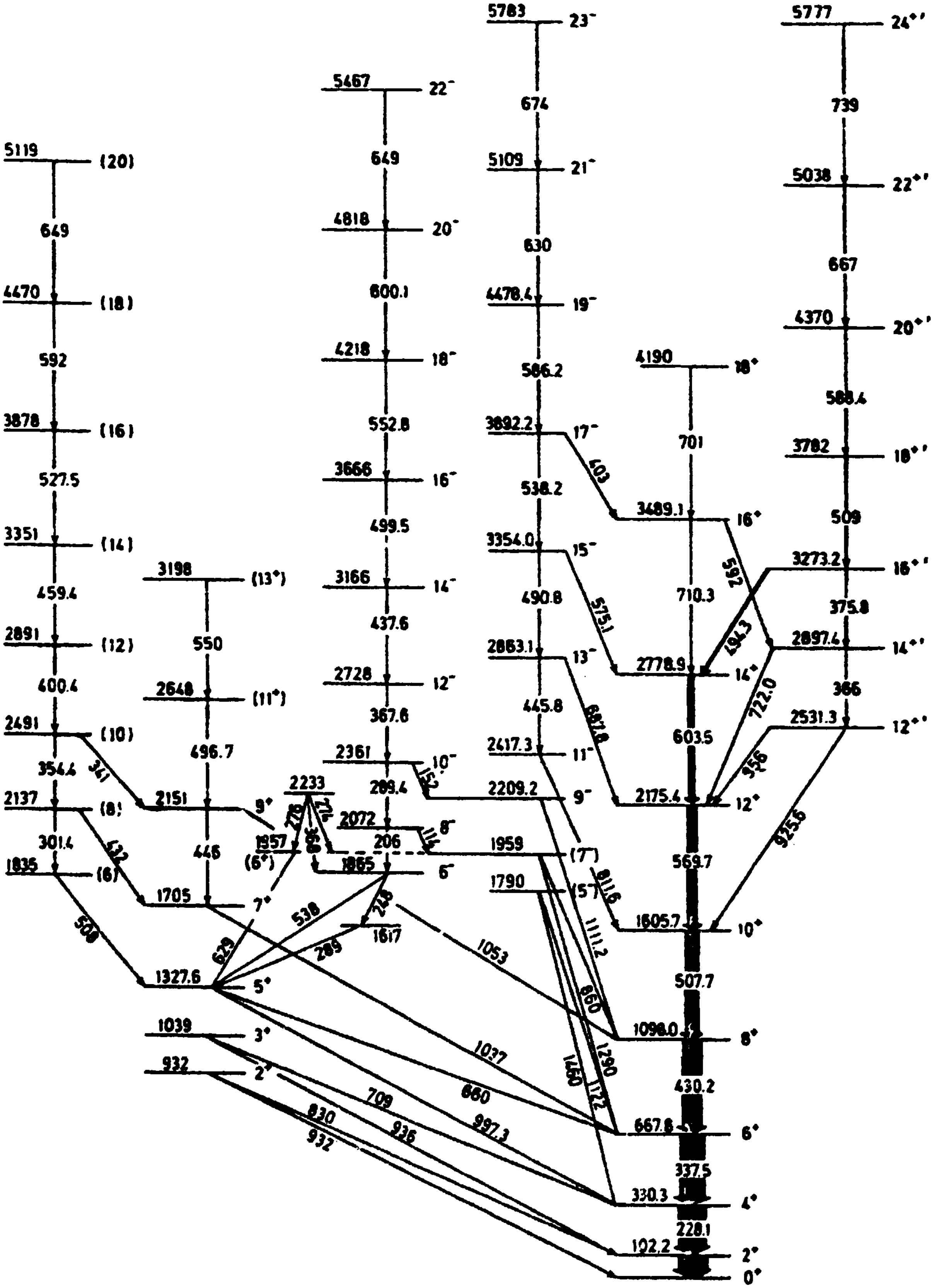
5783 23⁻
674
5109 21⁻
630
4478.4 19⁻
586.2
3892.2 17⁻
538.2
3354.0 15⁻
490.8
2863.1 13⁻
445.8
2417.3 11⁻
2209.2 9⁻
1959 (7⁻)
1790 (5⁻)
5467 22⁻
649
4818 20⁻
600.1
4218 18⁻
552.8
3666 16⁻
499.5
3166 14⁻
437.6
2728 12⁻
367.6
2361 10⁻
289.4
2072 8⁻
206
1865 6⁻
1617
5119 (20)
649
4470 (18)
592
3878 (16)
527.5
3351 (14)
459.4
2891 (12)
400.4
2491 (10)
354.4
2137 (8)
301.4
1835 (6)
3198 (13⁺)
550
2648 (11⁺)
496.7
2151 9⁺
446
1705 7⁺
2233
1957 (6⁺)
1327.6 5⁺
1039 3⁺
932 2⁺
4190 18⁺
701
3489.1 16⁺
710.3
2778.9 14⁺
603.5
2175.4 12⁺
569.7
1605.7 10⁺
507.7
1098.0 8⁺
430.2
667.8 6⁺
337.5
330.3 4⁺
228.1
102.2 2⁺
0⁺
5777 24⁺'
739
5038 22⁺'
667
4370 20⁺'
588.4
3782 18⁺'
509
3273.2 16⁺'
375.8
2897.4 14⁺'
366
2531.3 12⁺'
403
575.1
687.8
811.6
1111.2
860
1290
1460
1172
592
494.3
722.0
356
925.6
152
114
341
432
508
629
538
289
248
1053
1037
860
709
997.3
830
936
932
276
314
368

^{166}Yb

Fig. 3.

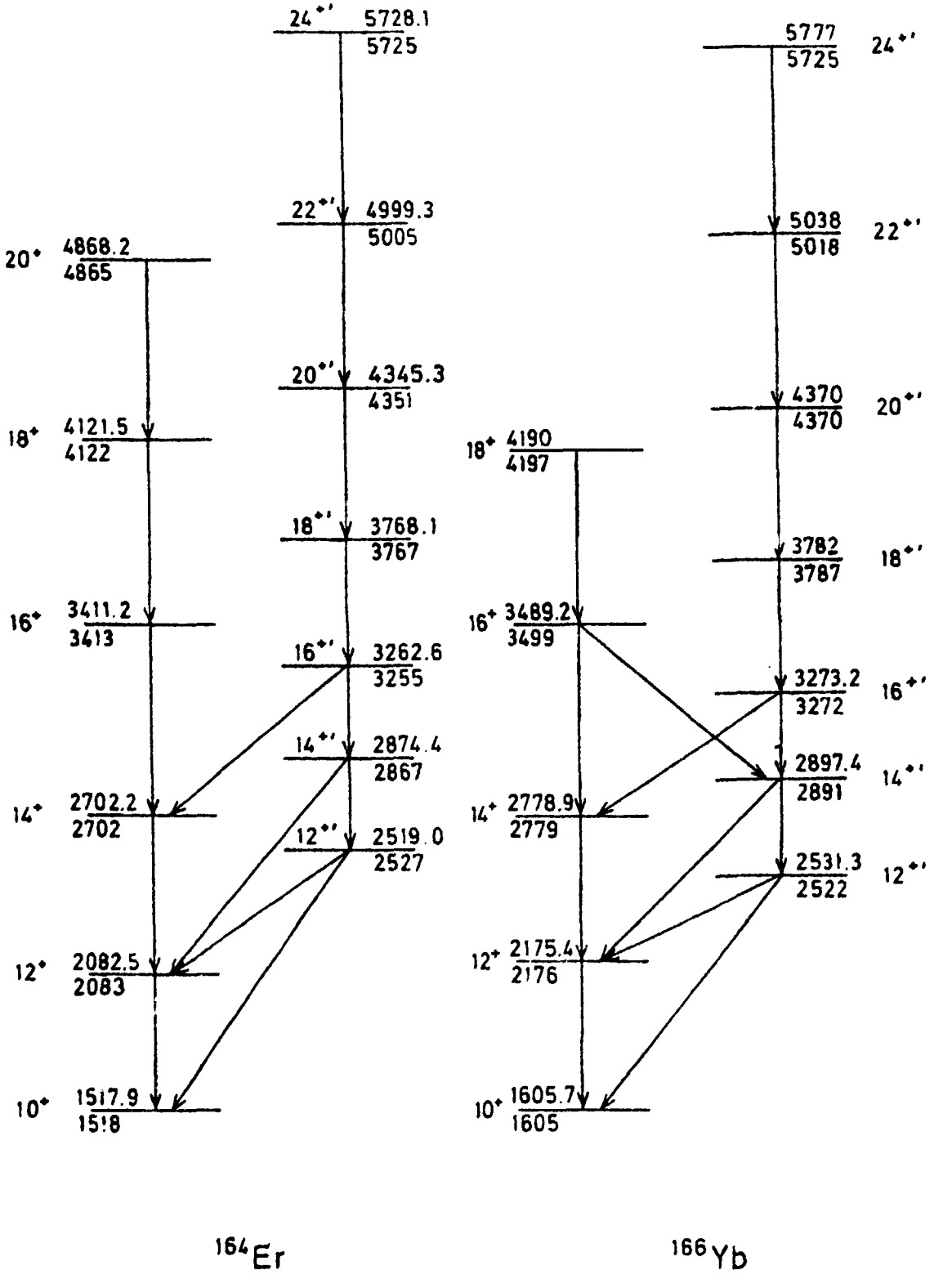
24+' 5728.1
5725
22+' 4999.3
5005
20+' 4345.3
4351
18+' 3768.1
3767
16+' 3262.6
3255
14+' 2874.4
2867
12+' 2519.0
2527
20+ 4868.2
4865
18+ 4121.5
4122
16+ 3411.2
3413
14+ 2702.2
2702
12+ 2082.5
2083
10+ 1517.9
1518
164Er
5777
5725
24+'
5038
5018
22+'
4370
4370
20+'
3782
3787
18+'
3273.2
3272
16+'
2897.4
2891
14+'
2531.3
2522
12+'
18+ 4190
4197
16+ 3489.2
3499
14+ 2778.9
2779
12+ 2175.4
2176
10+ 1605.7
1605
166Yb

Fig. 4

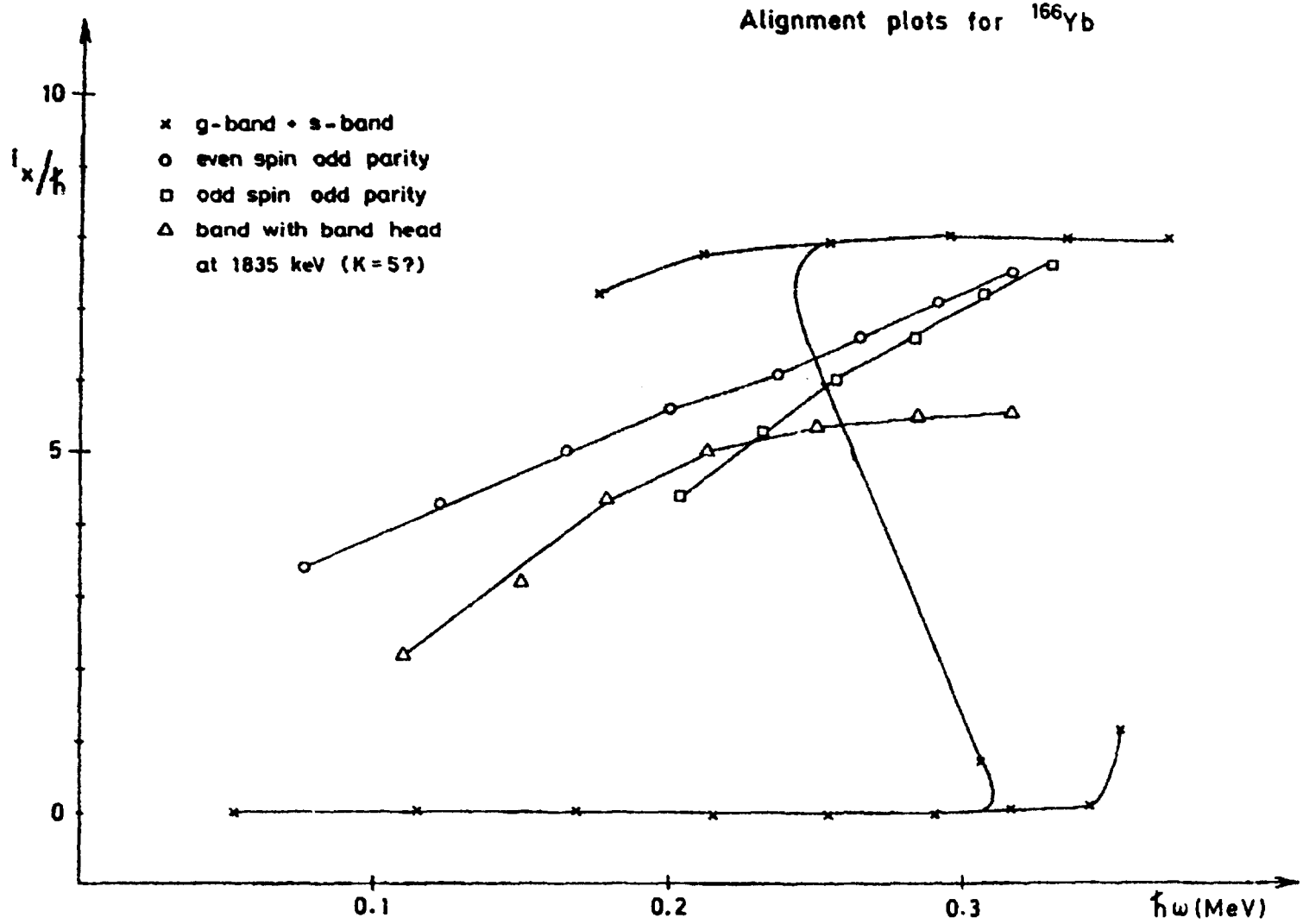
Alignment plots for ^{166}Yb
× g-band • s-band
o even spin odd parity
□ odd spin odd parity
△ band with band head at 1835 keV (K=5?)
$I_x/\hbar$
10
5
0
0.1
0.2
0.3
$\hbar\omega$ (MeV)

Fig. 5.

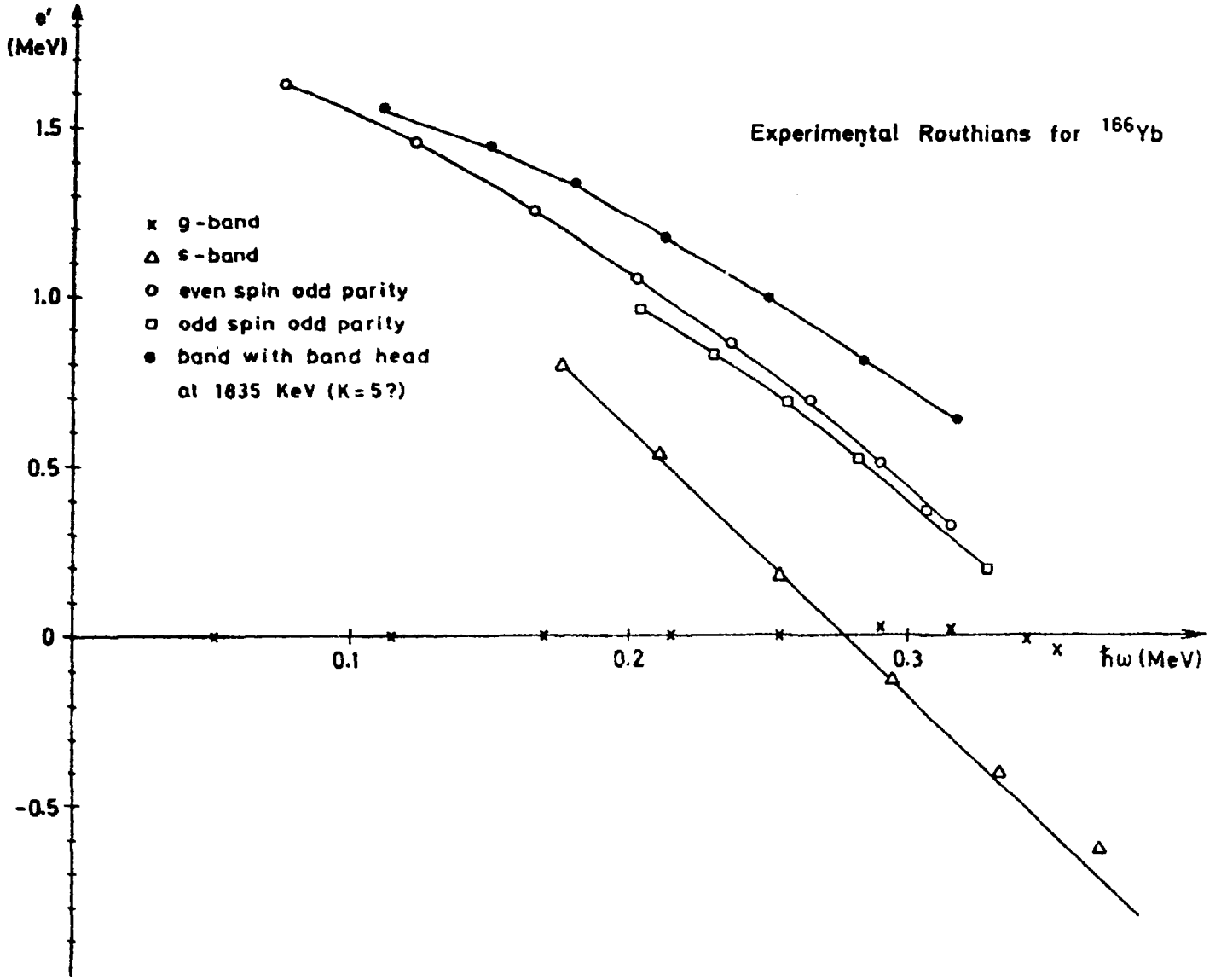
e'
(MeV)
1.5
1.0
0.5
0
-0.5
0.1
0.2
0.3
ħω (MeV)
Experimental Routhians for 166Yb
x g-band
Δ s-band
o even spin odd parity
□ odd spin odd parity
● band with band head
at 1835 KeV (K=5?)

Fig. 6.

Dokumentutgivare
UNIVERSITY OF LUND
Handläggare Department of Physics

Dokumentnamn
Internal report
Utgivningsdatum
1980-11-25

Dokumentbeteckning
LUNFD6/NFFK-7008)
Ärendebeteckning

Författare W. Waluś
N. Roy
S. Jónsson
L. Carlén
H. Ryde
G.B. Hagemann
B. Herskind
J.D. Garrett
Y.S. Chen
J. Almberger and G. Leander

Dokumenttitel och undertitel

HIGH-SPIN BAND STRUCTURE IN ^{166}Yb.

Referat (sammandrag)

High-spin states in ^{166}Yb have been studied via the ^{154}Sm(^{16}O,4n)^{166}Yb reaction with 80 MeV ^{16}O ions from the NBI tandem accelerator. γ-γ coincidence data were accumulated with an array of four Ge(Li) and four NaI(Tℓ) detectors to favour high multiplicity events. Totally about $3 \cdot 10^8$ events were accumulated in the coincidence experiment. Measurements of the angular distribution of the γ-radiation and the conversion coefficients were furthermore performed. Four weakly populated side bands are observed besides the yrast cascade which is followed up to its 24^+ member. The ground state band has thus been identified to its 18^+ state, while the crossing Stockholm band becomes the yrast band from its 16^+ member. The S-band is established from its 12^+ state. The observed level energies and transition rates are well reproduced in calculations within the particle rotor model.

Referat skrivet av
The authors.

Förslag till ytterligare nyckelord

Klassifikationssystem och -klass(er)

Indextermer (ange källa)

Omfång 20 pages +
6 figures

Övriga bibliografiska uppgifter

Språk
English

Sekretessuppgifter

ISBN
0348-9329

ISBN

Dokumentet kan erhållas från
Department of Cosmic and Subatomic Physics
University of Lund
Sölvegatan 14, S-223 62 LUND, Sweden.

Mottagarens uppgifter

Pris